

Pharmacokinetic/Pharmacodynamic model for antibacterial resistance in tuberculosis infection

Soumyadeep Chakraborty

School of Biological Sciences, National Institute of Science Education and Research, Bhubaneswar,
Khurda, Odisha 752050

Dr. Chetan J Gadgil

Chemical Engineering Division, National Chemical Laboratory, Dr. Homi Bhabha Road, Pune,
Maharashtra 411008

Table of Contents

Abstract

Abbreviations

1 INTRODUCTION

1.1 Background/Rationale

1.2 Statement of the Problems

1.3 Objectives of the Research

2 LITERATURE REVIEW

3 METHODOLOGY

3.1 Concepts

4 RESULTS AND DISCUSSION

4.1 SIMULATION OF THE MAXIMUM EFFECT (EMAX) MODEL OF BACTERIAL GROWTH

4.2 SIMULATION OF RESISTANCE EVOLUTION ON A GENE POOL OF BACTERIAL POPULATION

5 CONCLUSION AND RECOMMENDATIONS

5.1 Conclusion

5.2 Drawbacks

5.3 Scope for future research

REFERENCES

ACKNOWLEDGEMENTS

APPENDICES

The PBPK model

Pharmacokinetic/Pharmacodynamic model for antibacterial resistance in tuberculosis infection

Soumyadeep Chakraborty

School of Biological Sciences, National Institute of Science Education and Research,
Bhubaneswar, Khurda, Odisha 752050

Dr. Chetan J Gadgil

Chemical Engineering Division, National Chemical Laboratory, Dr. Homi Bhabha Road, Pune,
Maharashtra 411008

Abstract

Antibiotic use is very often a cause for a rise in antibiotic-resistant bacteria resulting in increased prevalence of infections. Modelling antibiotic resistance to estimate the pharmacodynamic effect of variable bacterial strains existing in cooperation inside the human body can be used to predict the drug dosage regimens for such infections. Bacteria may be intrinsically resistant to an antibiotic or may acquire resistance via de-novo mutations or horizontal transfer of resistance-conferring genes from other organisms due to selective pressure for survival upon the application of an antibiotic. The strains of resistant pathogens often have a lower growth rate and are less invasive or transmissible than the susceptible counterparts due to fitness cost associated with the maintenance of the resistance-conferring genes. In this project, a physiology based pharmacokinetic model is used to predict a time course tissue-specific concentration of a drug, Rifampin used for the treatment of disseminated pulmonary tuberculosis caused by the pathogen *Mycobacterium tuberculosis*. Rifampin acts on the pathogen by preventing nucleic acid synthesis through inhibition of DNA-dependent RNA polymerase activity. *M. tuberculosis* upon antibiotic exposure also exhibits increased formation of antibiotic-tolerant cells called persister cells showing decreased or no metabolic activity and thus may act as a reservoir of viable cells capable of resuscitation and mutation into resistant cells upon a drop in intracellular drug concentration. The data obtained is used to establish a

complex relationship between drug exposure and the emergence of antibiotic resistance using first-order ordinary differential equations (ODEs). Further, the simulation of time-kill curves in various organs is done from the intracellular drug concentration data obtained from pharmaco-kinetic modelling using SimBiology. The objective is to build drug dose strategies that can minimize the dissemination of resistance and to further anticipate the impact of these strategies.

Keywords or phrases: *M. tuberculosis*, Mathematical model, Resistance, Pharmacokinetic, Pharmacodynamics

Abbreviations

Abbreviations

TB	Tuberculosis
MIC	Minimum Inhibitory Concentration
CFU	Colony Forming Units
MDR	Multi Drug Resistant

1 INTRODUCTION

1.1 Background/Rationale

Individuals with weak immune system are often not able to contain a pathogenic infection to its initial locus in the human body. One such chronic infection, Tuberculosis caused by the bacterial pathogen *Mycobacterium tuberculosis* may invade multiple organs of the human body though it primarily affects the lungs. Disseminated TB occurs within weeks of primary infection and can spread either through blood or via the lymphatic system of the human body. Though latent tuberculosis shows little or no symptoms, in active pulmonary and extrapulmonary tuberculosis the symptoms are occasionally nonspecific with variable durations that may include long-standing cough and soreness of the throat rarely with blood refluxes, chest pains, tiredness, fever, weight loss, profuse sweating at night, loss of appetite, etc., along with a few localization specific symptoms such as abdominal pain and jaundice in case of hepatic tuberculosis. A definitive diagnosis of the bacterial manifestation and growth is very difficult and mostly relies on histopathological tests such as a biopsy of internal organs and tissues. We gather from the literature of several clinical journals that it is difficult to

obtain a clinical diagnosis of bacterial growth in patients through repeated physical tests or visual examinations for attenuation of symptoms as a proportion of bacterial cells is often unresponsive to drug effects and remain dormant but shows phenotypic effect in absence of drug (1,2,3).

In such context, mathematical modelling combined with microbiological experiments may prove to be a powerful tool to help physicians and public health practitioners to examine the course of dissemination of the disease, predict the optimum drug dose regimen and further assess the efficacy of such dosage programmes. In this project a Physiology based Pharmacokinetic (PBPK) model built previously on MatLab Sim-Biology GUI based on the model equations provided by Zurlinden et. al. (4) is further modified to include the kinetics for drug action and resistance development of *M. tuberculosis* during repeated oral administration of a very effective anti-tuberculosis drug, Rifapentine. Rifapentine acts on the transcription process of the bacterial genome by inhibiting the DNA-dependent RNA polymerase activity through inactivation of bacterial RNA polymerase but does not affect the mammalian counterpart of the enzyme. The parameter values for simulation are either obtained from literature or are estimated based on the trend followed by similar bacterial species due to unavailability of experimental data. The result inferred by examining these trends can be utilised to construct an optimum drug dosing strategy to kill all susceptible cells and limit the growth of the resistant generations.

1.2 Statement of the Problems

There is no available analytical/statistical growth model of drug-resistant species of *Mycobacterium tuberculosis* and action of Rifapentine on extra-pulmonary tuberculosis infection. The following research aims to address these problems and further improve on the prevalent drug dosage models for Rifapentine. In this experiment, data obtained from literature is used as an ideal estimate for parameters to simulate growth-kill curves.

1.3 Objectives of the Research

This research aims to establish an analytical growth model for the drug-resistant species of *M. tuberculosis* and how it is affected through the pharmacodynamic action of the drug Rifapentine. This would be beneficial to estimate the required quantity of drug for individual suffering of extrapulmonary tuberculosis infection based on his/her physiology to prevent either excess drug intake that may result in toxicity or reduced drug intake that may result in a relapse of bacterial growth and drug resistance.

2 LITERATURE REVIEW

A PBPK model was previously made in the lab using Matlab Simbiology based upon the data obtained from the work of Zurlinden et. al. (4). PBPK models are multi-compartment models where each compartment corresponds to different organs or tissues interconnected through blood or lymph flow. A PBPK model allows for tissue-specific concentration profiling of drug ADME both at the major site of action for the antibiotic effect of the drug and also other sites of potential toxicity. Previously models developed on rodents based upon experimental data by Lyons et. al.(5) and Zhang et.(6) al. for disposition of Rifampin in various compartments for tuberculosis infection (Fig. 1) and comparison of the same to time based experimental observation in murine species provides strong evidence about the effectiveness of PBPK models in determination of time course drug distribution.

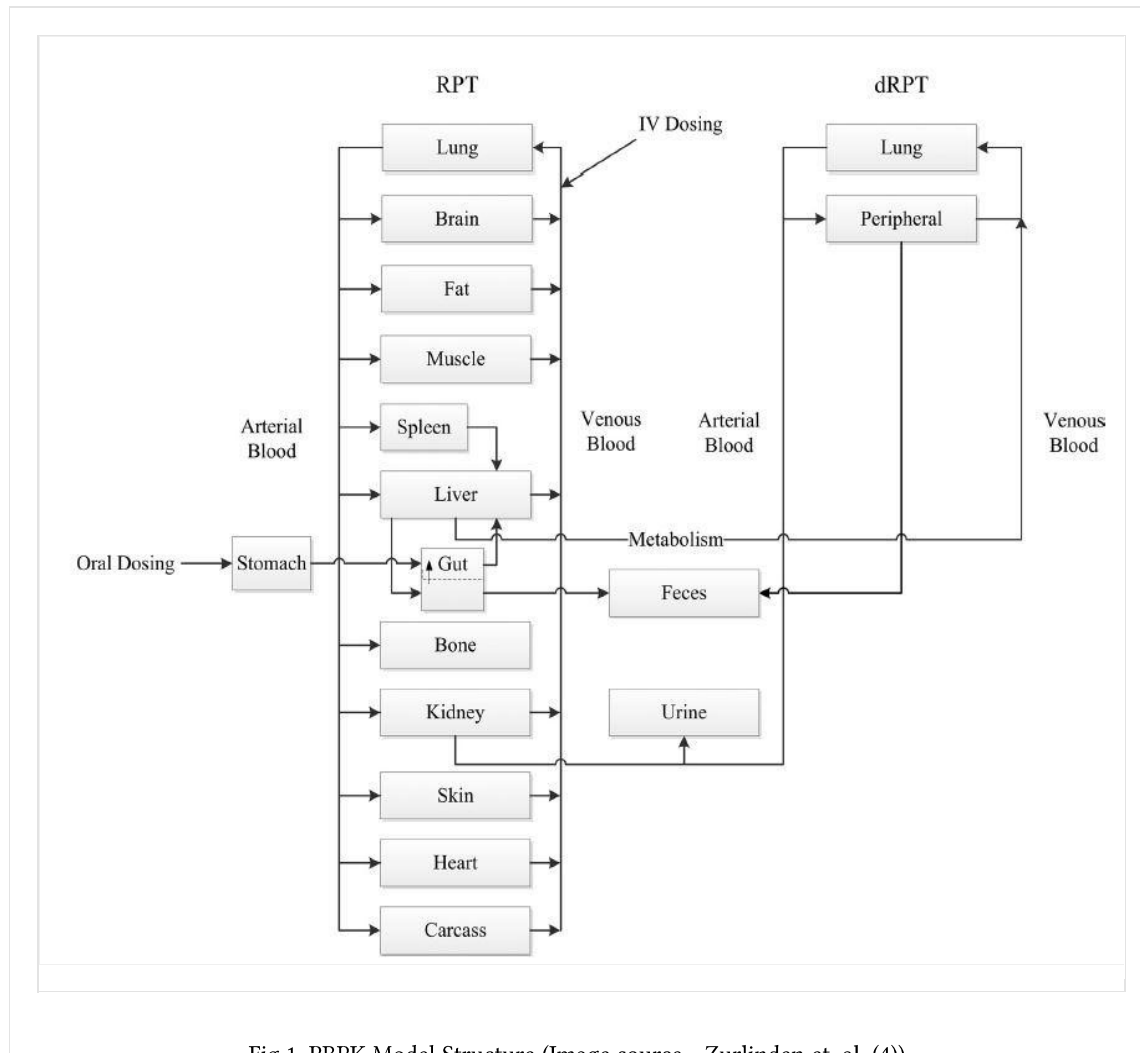


Fig 1 PBPK Model Structure (Image source - Zurlinden et. al. (4))

Pharmacokinetic models when integrated with pharmacodynamic (PD) models can be used to analyse drug effects on the bacterial population in vivo as it is difficult to carry periodic estimation of the same through scheduled extraction of tissue from different organs of a live organism. Most of the articles available in literature employ the use of the maximum effectivity model (or Zhi model) for the effect of the drug on bacterial population (7,8,9,10). The affinity of the drug for the receptor is described by the EC₅₀, the concentration of the drug required to give a half-maximal response. The Emax model is given by the equation :

$$R = E_0 + \frac{D \times E_{max}}{D + EC_{50}} \quad (1)$$

The drug concentration-effect relationship is described by the same function as the enzyme velocity-substrate concentration relationship. E₀ is the basal effect when the dose of the drug is zero. R is the effect at drug concentration D, Emax is the maximal effect at high drug concentrations when all the receptors are occupied by the drug, and EC₅₀ is the drug concentration to give the half-maximal effect.

Davies et. al. (11) experimentally proved that the origin and evolution of the resistant population is the primary cause of drug action failure as it allows bacteria to sustain in elevated drug concentration. Survivability of resistant cell demands increased energy requirements due to fitness cost associated with mutation or production of surplus proteins to bypass high drug concentration levels (12). As shown by Weisch et. al. (12), sometimes compensatory mutations occurring in a separate gene locus can lower the fitness cost to make the resistant cells capable of survival in competition with sensitive cells under external phenotypic pressure. Another recent article by Fisher et. al.(13) exhibited the presence of a small population of dormant/persister cells in the niche of antibiotic sensitive cells that can survive in minimum or no resources and having zero growth rate to form an effective reservoir of potentially infectious bacterial cells capable of resuscitation under depleted drug concentration levels. Further, Sebastian et. al. (14) proved the emergence of persister population in cells of *Mycobacterium tuberculosis* against tuberculosis drugs. A much lesser amount of research had been done to prove the phenomenon of phenotypic tolerance, apart from an article by Wiuff et. al. (7) which showed that a fraction of bacterial cells can also be inherently resistant to usually sub-lethal level of antibiotic concentration and may exhibit higher MICs. Also, as shown by Ankomah and Levin (9), the innate immune response is also a major contributing factor in the elimination of all types of bacterial strain and in collaboration with effective drug treatment can completely eliminate the bacterial population in a living system. They also demonstrated the use of multi-drug therapy (Ankomah, Peter and Levin (15)) for effective treatment as a secondary drug can be used to kill the primary drug-resistant population by not allowing sufficient time to mutate and adapt to multiple drugs. In most cases, drug action and evolution of the multiple aforementioned strains of bacteria depends on the variable drug concentration levels and also the drug type as different drugs would have a

different target system for its action. One such drug, Rifapentine is very effective against *M. tuberculosis* as it affects transcription through inhibition of bacterial polymerase enzyme and has no effect on the mammalian counterpart. Since, a limited amount of parametric data is available for growth and mutation of *M. tuberculosis* under the application of Rifapentine most of the simulations in this project is based on an ideal estimate of parameter values according to other Mycobacterial species (Ankomah, Peter and Levin (15)). We develop on a recent article by Windels et. al. (10) to propose an ideal model for drug action on the phenotypically different strains of *M. tuberculosis*. Most of the research on drug action extensively uses the sigmoid Emax (maximum effect) model as an ideal model for drug action that takes into account the minimum inhibitory concentration and growth rate of *M. tuberculosis* under selection pressure.

3 METHODOLOGY

3.1 Concepts

The Pharmacokinetic model for drug distribution is based on equations of first-order reaction kinetics where most of the parameters are obtained as experimental observations and some are estimated statistically through a hierarchical Bayesian framework and Markov Chain Monte Carlo simulations (MCMC)(see appendix). Pharmacodynamic model of drug action on the bacterial population is based upon the parameter estimates obtained from experimental data by Ankomah and Levin. The assumptions made are as follows :

3.1.1 Assumption A

The growth rate of the sensitive population (S) is logistic and is limited by the ratio of the total number of cells (N_t) to the carrying capacity (K) of each organ. The growth rate of the resistant population (R) is less than that of the sensitive population due to fitness costs of mutation and shows very limited or zero death rate due to antibiotic application. Persistent cells, on the other hand, are dormant and have a very slow or zero growth rate with the capability to survive antibiotic application.

$$\frac{dS}{dt} = \left(1 - \frac{N_t}{K}\right) gmax(S) \times S \quad (2)$$

$$\frac{dR}{dt} = \left(1 - \frac{N_t}{K}\right) gmax(R) R \quad (3)$$

3.1.2 Assumption B

To simulate the drug action on the sensitive population, a sigmoidal Emax model is used. In saturated drug levels, the population exhibits a negative growth rate (g_{min}) as the number of death per generation is greater than the number of divisions. As the drug concentration decreases, the growth rate increases as the drug-mediated kill rate (δ_S) tend to zero.

$$\frac{dS}{dt} = \left(1 - \frac{N_t}{K}\right)(gmax(S) \times S - \delta_S S) \quad (4)$$

$$\square \delta_S = \frac{\left(gmax - gmin\right)\left(\frac{A}{zMIC}\right)^k}{\left(\frac{A}{zMIC}\right)^k - \frac{gmin}{gmax}} \quad (5)$$

3.1.3 Assumption C

There is a constant rate of mutation from the sensitive to the resistant population. The first part of the mutation rate represents the intrinsic rate of mutation in absence of the drug while the second part represents the increase in the rate of mutation due to selection pressure in presence of the drug.

$$\frac{dS}{dt} = \left(1 - \frac{N_t}{K}\right)(gmax(S) - \delta_S S) - \mu_W S(t) \quad (6)$$

$$\frac{dR}{dt} = \left(1 - \frac{N_t}{K}\right)gmax(R)R + \mu_W S(t) \quad (7)$$

$$\square \mu(t) = mg(A) + \tau me^{-hg(A)} \quad (8)$$

3.1.4 Assumption D

A portion of both sensitive and resistant cells enters the dormant phase to survive the antibiotic effect. Persistent cells are capable of resuscitation into both sensitive and resistant

cells and thus acts as a reservoir of infectious cells. A fraction of the Wild Type persister cells (P_W) also mutate to form Resistant persistent cell (P_R).

$$\frac{dS}{dt} = (1 - \frac{N_t}{K})(gmax(S) - \delta_S S) - aS(t) + bP_W(t) - \mu_W S(t) \quad (9)$$

$$\frac{dR}{dt} = (1 - \frac{N_t}{K})gmax(R)R - aR(t) + bP_R(t) + \mu_W S(t) \quad (10)$$

$$\frac{dP_W}{dt} = aS(t) - bP_W(t) - \mu_P P_W(t) \quad (11)$$

$$\frac{dP_R}{dt} = aR(t) - bP_R(t) + \mu_P P_W(t) \quad (12)$$

3.1.5 Assumption E

Innate immune cells (E) acts on all three types of cells, though the immune response is lower for the resistant and persistent bacterial population as in comparison to the sensitive population. A constant rate of recruitment and inactivation of immune cells is observed in this simulation.

$$\frac{dS}{dt} = (1 - \frac{N_t}{K})(gmax(S) \times S - \delta_S S) - aS(t) + bP_W(t) - \mu_W S(t) - j_N S(t)E(t) \quad (13)$$

$$\frac{dR}{dt} = (1 - \frac{N_t}{K})gmax(R)R - aR(t) + bP_R(t) + \mu_W S(t) - j_N R(t)E(t) \quad (14)$$

$$\frac{dP_W}{dt} = aS(t) - bP_W(t) - \mu_P P_W(t) - j_P P_W(t)E(t) \quad (15)$$

$$\frac{dP_R}{dt} = aR(t) - bP_R(t) + \mu_P P_W(t) - j_P P_R(t)E(t) \quad (16)$$

$$\square \frac{dE}{dt} = q(emax - E(t)) - lE(t) \quad (17)$$

3.1.6 Assumption F

Tolerance is modelled as a fraction of sensitive population resistant to certain levels of drug concentration exhibiting a higher MIC. There exists a probability (f) that at each division the new sister cells would be tolerant to the given drug concentration level. The growth rate of tolerant cells (T) may be either lower or equal to that of the sensitive cells.

$$\begin{aligned} \frac{dS}{dt} &= (1 - \frac{N_t}{K})\{(1 - f)(gmax(S) \times S + gmax(T) \times T) - \delta_S S\} - aN_W(t) + bP_W(t) - \mu_W N_W(t) - j_N \\ &\quad N_W(t)E(t) \end{aligned} \quad (18)$$

$$\frac{dT}{dt} = (1 - \frac{N_t}{K})\{f(gmax(T) \times T + gmax(S) \times S)\} - aN_W(t) + bP_W(t) - \mu_W N_W(t) - j_N N_W(t)E(t) \quad (19)$$

where,

$$N_W = S + T \quad (\text{Number of Sensitive cells} + \text{Number of Tolerant cells}) \quad (20)$$

3.1.7 Assumption G

Some portion of the resistance cells shows further mutation which may be either compensatory mutation or a random mutation in a separate locus such that the cells loses its resistance. Here, we assume that the mutation leads to loss of resistance but the frequency of such mutations are so low that we neglect the increase for the number of sensitive cells. Thus ideally, the rate of growth of all the different phenotypic strains can be represented by the following systems of differential equations :

$$\begin{aligned}
 \frac{dS}{dt} &= (1 - \frac{N_t}{K})\{(1 - f)(g_{max}(S) \times S + g_{max}(T) \times T) - \delta_S S\} - aN_W(t) + bP_W(t) - \mu_W N_W(t) - j_N N_W(t)E(t) \\
 \frac{dT}{dt} &= (1 - \frac{N_t}{K})\{f(g_{max}(T) \times T + g_{max}(S) \times S)\} - aN_W(t) + bP_W(t) - \mu_W N_W(t) - j_N N_W(t)E(t) \\
 \frac{dP_W}{dt} &= aN_W(t) - bP_W(t) - \mu_P P_W(t) - j_P P_W(t)E(t) \\
 \frac{dP_R}{dt} &= aN_R(t) - bP_R(t) + \mu_P P_W(t) - \mu_P P_R(t) - j_P P_R(t)E(t) \\
 \frac{dR}{dt} &= (1 - \frac{N_t}{K})g_{max}(R)R - aN_R(t) + bP_R(t) + \mu_W N_W(t) - \mu_R N_R(t) - j_N N_R(t)E(t)
 \end{aligned} \tag{21}$$

We exclude the assumptions D, F and G for the dynamics of formation of tolerant and persister cells in this model due to a lack of experimental data. Nevertheless, the model includes the equations for all the above bacterial species and respective simulations can be obtained with the input of suitable parametric data.

Table 1 Parameters used in the given model

PARAMETERS		VALUE	SOURCE
SYMBOL	NAME		
$g_{max}(S)$	maximum bacterial growth rate of sensitive cells in absence of the drug	0.0453 hr ⁻¹	Ankomah,Peter and Levin (15)
$g_{max}(T)$	growth rate of tolerant cells	Not used in this model	—
δ_s	death rate of sensitive population	Variable under drug concentration	—
C	carrying capacity (Resource-limited growth)	1500 CFU/ml in each tissue	Estimated
a	persister formation rate	Not used in this model	—
b	resuscitation rate of persister population	Not used in this model	—
μ_w	mutation rate of wild type population	Variable under drug concentration	—
μ_p	mutation rate of persister population	Not used in this model	—
μ_r	mutation rate of resistant population	Not used in this model	—
k	hill constant	0.925	Ankomah,Peter and Levin (15)
j_p	immune mediated killing rate of persister cells	5×10^{-8} hr ⁻¹	Windels et. al. (10)

j_n	immune mediated killing rate of WT and resistant cells	$5 \times 10^{-6} \text{ hr}^{-1}$	Windels et. al. (10)
f	probability that the new bacterial cell is tolerant		
$z\text{MIC}$	Minimum Inhibitory concentration of the drug	1.27 mg/L	Ankomah,Peter and Levin (15)
g_{\min}	minimum bacterial growth rate at saturated drug concentration	-0.125 hr^{-1}	Ankomah,Peter and Levin (15)
$g_{\max}(R)$	growth rate of resistant cells	0.040 hr $^{-1}$	Estimated
A	drug concentration	Variable	—
q	rate of recruitment of effector cells	$3 \times 10^{-4} \text{ hr}^{-1}$	Windels et. al. (10)
τ	maximum fold increase in mutation rate in presence of antibiotics	2	Windels et. al. (10)
m	rate of mutation	$10^{-4} - 10^{-5} \text{ per division}$	Windels et. al. (10)
h	constant for increase in mutation in presence of antibiotics	5	Windels et. al. (10)
e_{\max}	maximum density of effector cells in the reservoir	10^6	Windels et. al. (10)
l	rate of inactivation of effector cells	10^{-3} hr^{-1}	Windels et. al. (10)

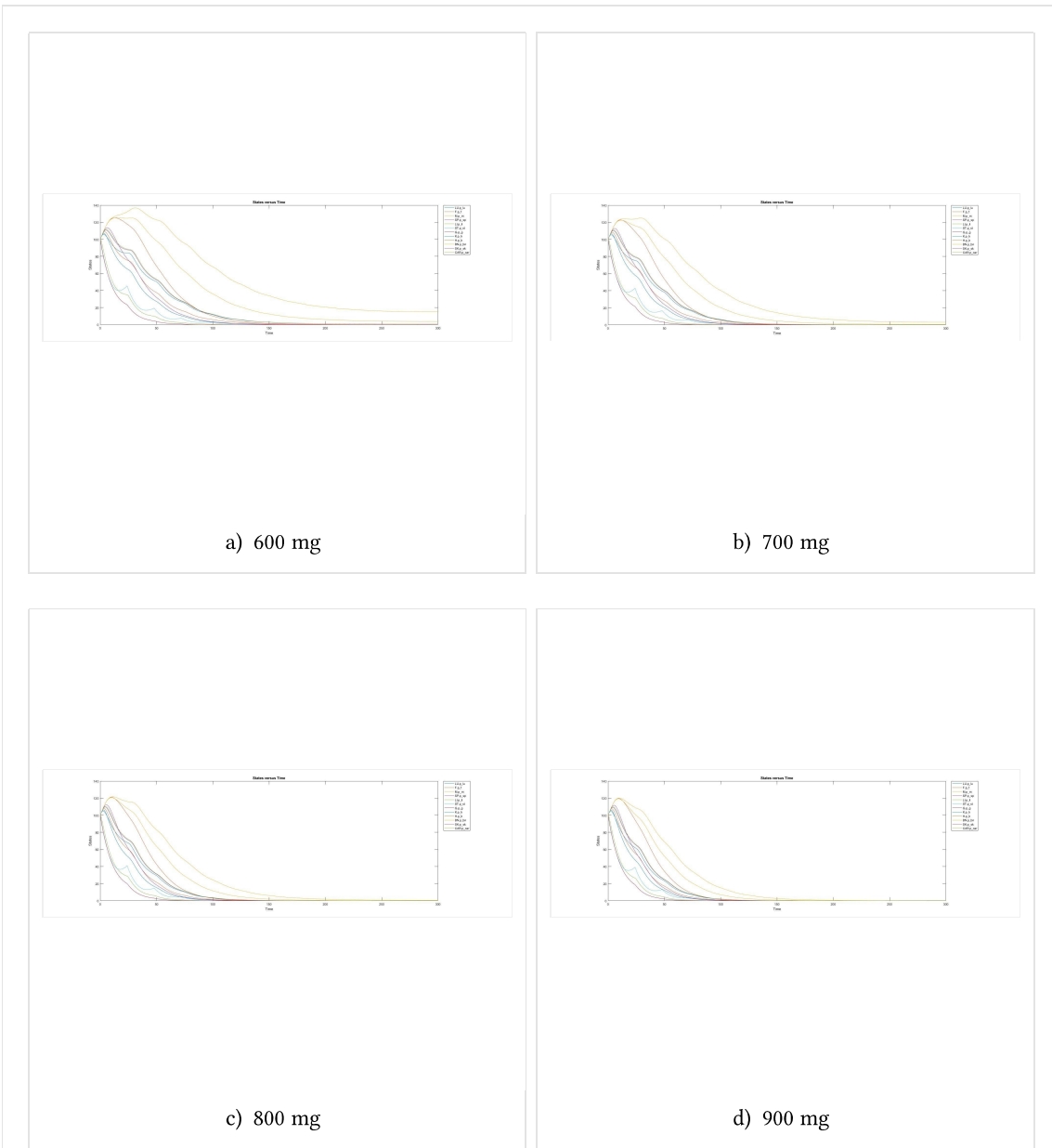
4 RESULTS AND DISCUSSION

4.1 SIMULATION OF THE MAXIMUM EFFECT (EMAX) MODEL OF BACTERIAL GROWTH

For the preliminary assessment, the pharmacodynamics of the time-kill effect of the drug is plotted based on its pharmacokinetics. We use the Emax model of drug action to find the dynamics of the change in the bacterial population in response to a change in the following experimental conditions.

4.1.1 Change in drug concentration

The results obtained are as follows :



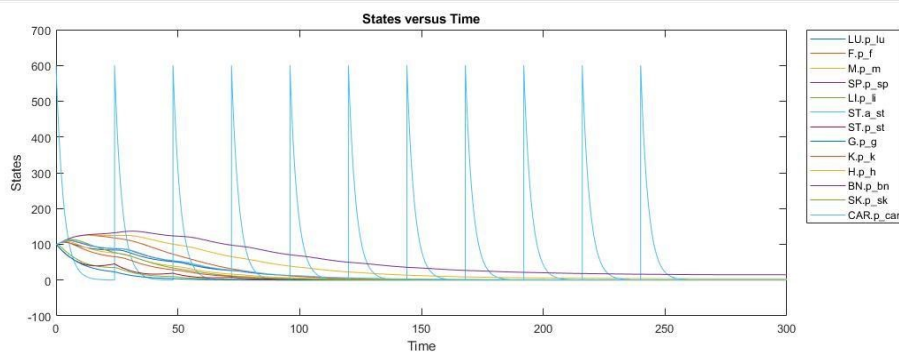
initial concentration of sensitive bacterial cells in each compartment is kept constant at 100 CFU/ml)

Inference

The observation of an elevated decay rate at higher drug concentration is trivial because its anticipated that drugs are antagonistic to some specific bacterial cell proteins and thus higher drug level would lead to a higher probability of drug-bacterial interaction leading to an increased death rate. It has been proved that humans can tolerate high levels of Rifapentine and the threshold for toxicity is as high as dosages equivalent to 12-15 mg (1). Thus, it is safe to administer higher doses of Rifapentine to reach elevated drug levels in tissues for more rapid suppression of symptomatic effects owing to an elevated decay rate of bacterial cells.

4.1.2 Change in the interval duration of each repetitive drug dosage

The results obtained are as follows :



a) 24 hrs Interval between each drug dosage of 600mg

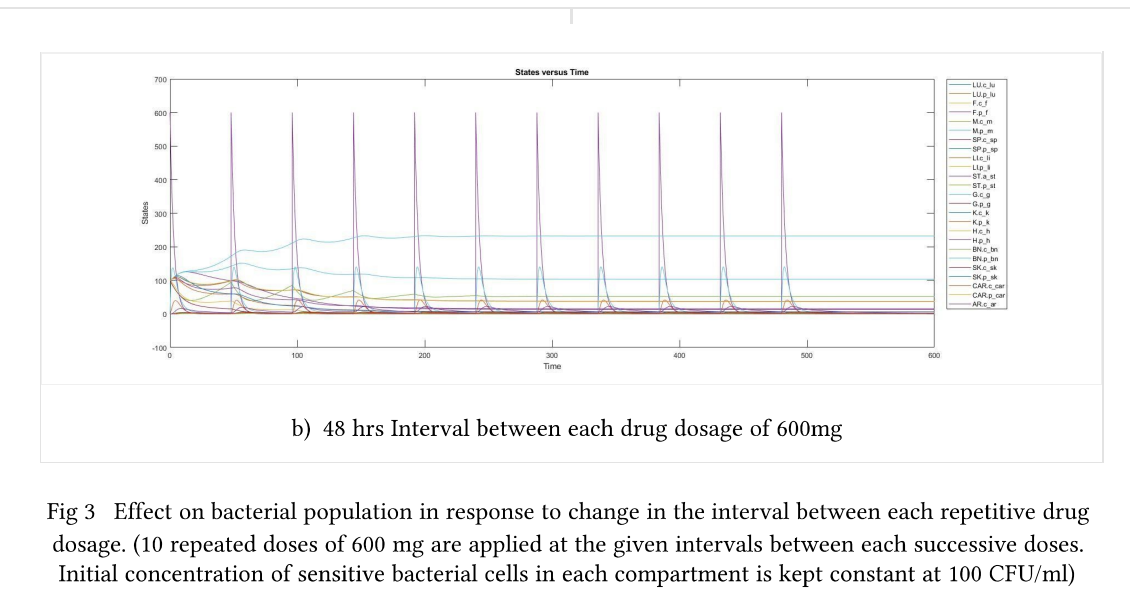


Fig 3 Effect on bacterial population in response to change in the interval between each repetitive drug dosage. (10 repeated doses of 600 mg are applied at the given intervals between each successive doses. Initial concentration of sensitive bacterial cells in each compartment is kept constant at 100 CFU/ml)

Inference

As observed from the graph, a greater duration of interval between each repetitive doses doesn't allow the retainment of the drug in sufficient amount as to facilitate decay of sensitive bacterial cells in most of the compartments and thus leads to treatment failure. Drugs once ingested is absorbed through the bloodstream into different organs and is progressively excreted or removed via the veins and capillaries while some part of it is constantly metabolised. Given the pharmacokinetic property of Rifapentine, a more stringent dosage schedule should be devised that permits the retainment of sufficient drug amount in the tissues until the ingestion of successive drug dose.

4.1.3 Change in number of repeated drug dosage

The results obtained are as follows :

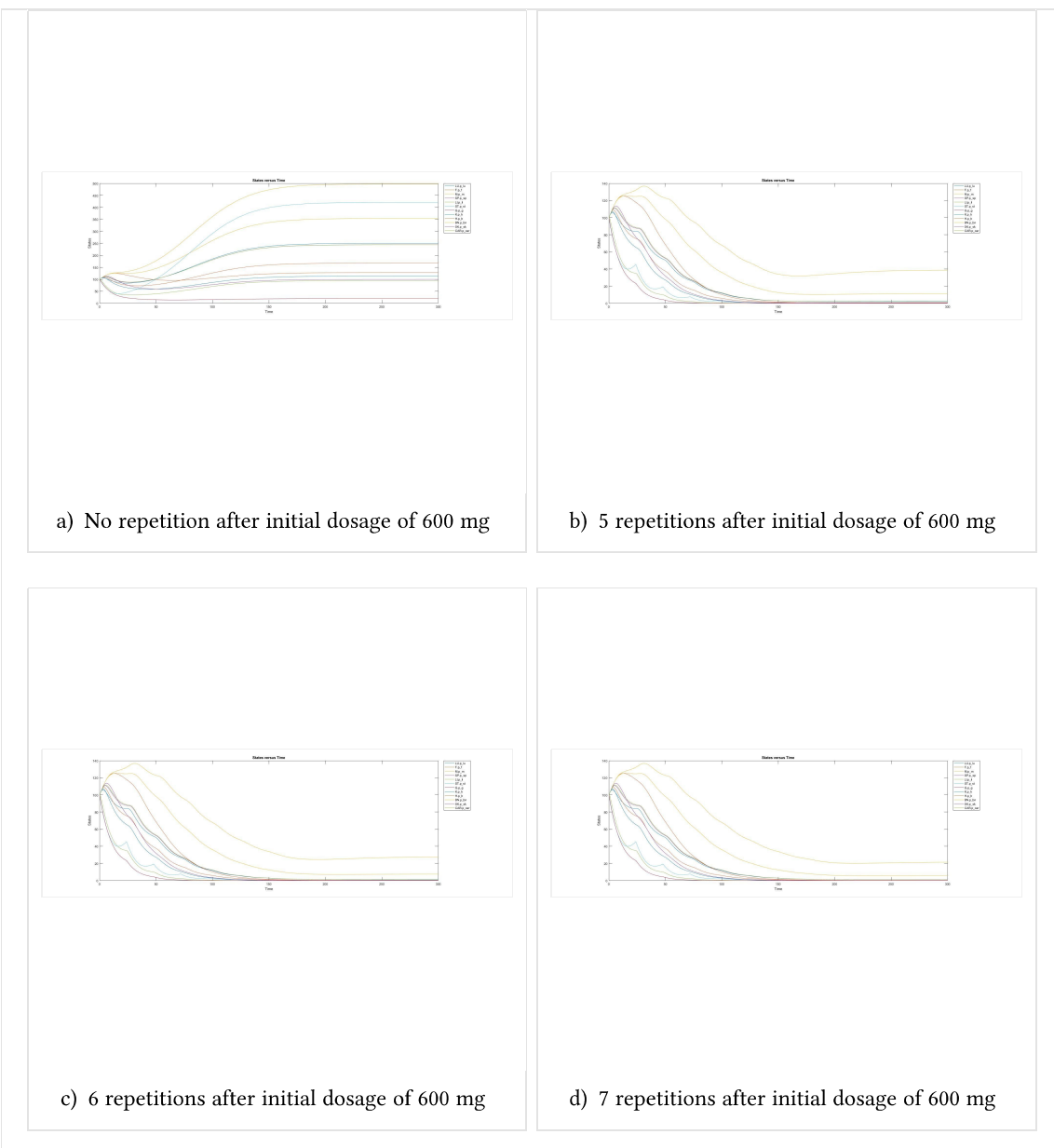


Fig 4 Effect on bacterial population in response to change in the number of repetitive drug dosage . (Doses of 600 mg concentration is applied at an interval of 24 hrs between each successive doses for the given number of repetitions. The initial concentration of sensitive bacterial cells in each compartment is kept constant at 100 CFU/ml)

Inference

From the observations obtained in the given simulation and from the data of the former simulations, an optimum dosage schedule can be deduced that employs the optimum number of drug dosages required to suppress all of the sensitive bacterial population present in each compartment. As observed more repetitions allows greater retainment of the drug in each tissue until the concentration of bacterial cells reaches a minimum boundary concentration, not capable of phenotypic expression sufficient enough to produce symptomatic effects in the patient. Hence an ideal drug dosage regime should take account the number of doses, concentration of each dose and number of repetition between each successive doses.

4.2 SIMULATION OF RESISTANCE EVOLUTION ON A GENE POOL OF BACTERIAL POPULATION

To the given Pharmacodynamic model of drug action, we further simulate and analyse the evolution of bacterial resistance and action of immune response on both strains of the bacterial population. As anticipated, the model exhibits logistic growth for resistant bacterial cells post mutation and multiplication from a stock of sensitive cells. Resistant cells exhibit a lower rate of multiplication due to compensation of fitness cost of energy associated with the acquisition of resistance. Based on an article by Telenti et. al. (17), it is found that mutation in a small segment of the *rpoB* gene is associated with accumulation of resistance to Rifapentine. The length of the gene is around 3.5 kBP and the associated mutation rate for *M. tuberculosis* is significantly less as compared to other first-line anti-TB drugs. The immune response which largely comprises the innate immunity containing phagocytes, mast cells, T cells, macrophages and the granulocytes provides a major contributory effect in terms of immune-mediated death of bacterial cells. Thus a strong immune response in association with optimum drug treatment regimen may be very effective to curb the growth and evolution of phenotypically drug-resistant and tolerant bacterial cells. The contributory effect of immunity may be highlighted through the simulations given below :

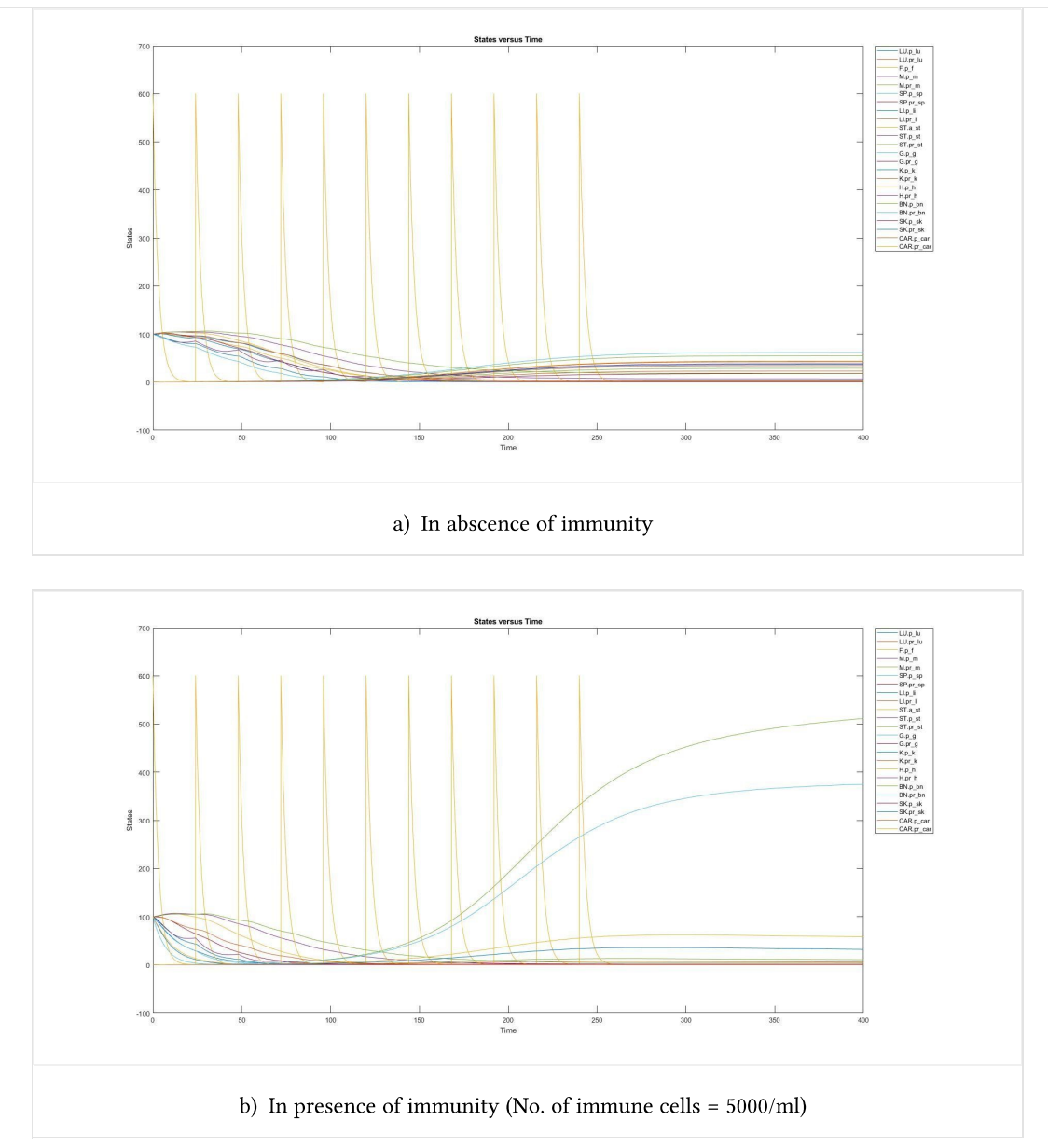
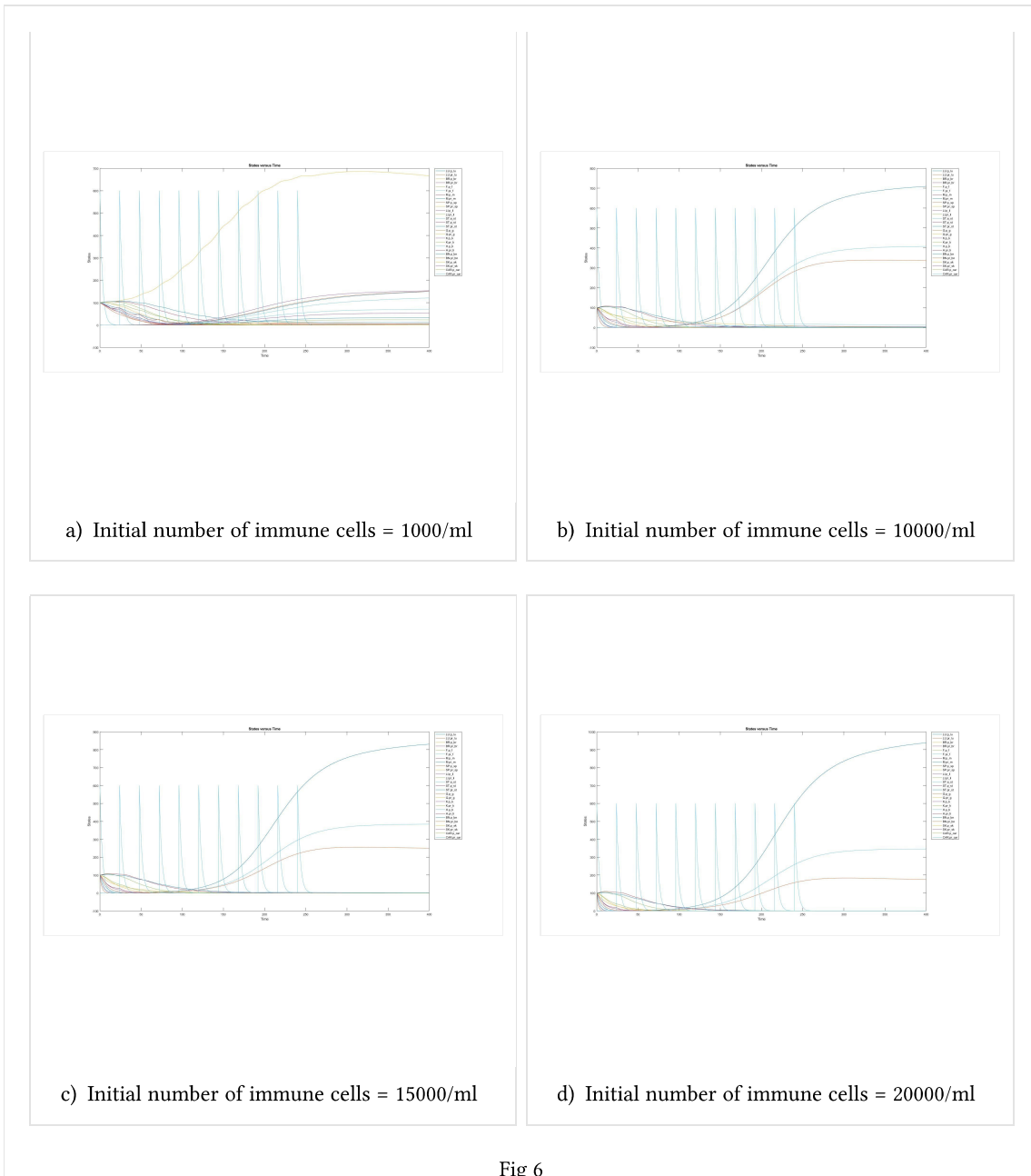


Fig 5 Growth of sensitive and resistant population in the presence and absence of immunity. (10 repeated doses of 600 mg concentration applied at an interval of 24 hrs between each successive doses. The initial concentration of sensitive and resistant bacterial cells in each compartment is kept constant at 100 CFU/ml and 0 CFU/ml respectively)

4.2.1 Dynamics of population growth with change in initial number of immune cells

The results obtained are as follows :



Dynamics of population growth with change in the initial number of immune cells. (10 repeated doses of 600 mg concentration applied at an interval of 24 hrs between each successive doses. Initial concentration of sensitive and resistant bacterial cells in each compartment is kept constant at 100 CFU/ml and 0 CFU/ml respectively)

Inference

The given observation shows that a higher number of immune cells are capable of accelerating the kill rate of sensitive cells by complementing the drug effect. A higher immune cell count is also effective in the complete suppression of resistant population growth in multiple compartments, the reason for which is lack of opportunity to mutate and grow for the sensitive gene pool as the decay rate is much higher. Hence, we can infer that higher immune cell count provides stronger resistance in an individual to a disease outbreak. Few organs in the presence of higher immune cell counts continue to exhibit a logistic growth owing to a very less concentration of drug present in those compartments, providing little or no impact to the rate of mutation and growth of sensitive cells.

4.2.2 State of infection and effect on bacterial population when the initial dosage is applied at a time lag post onset of infection

The results obtained are as follows :

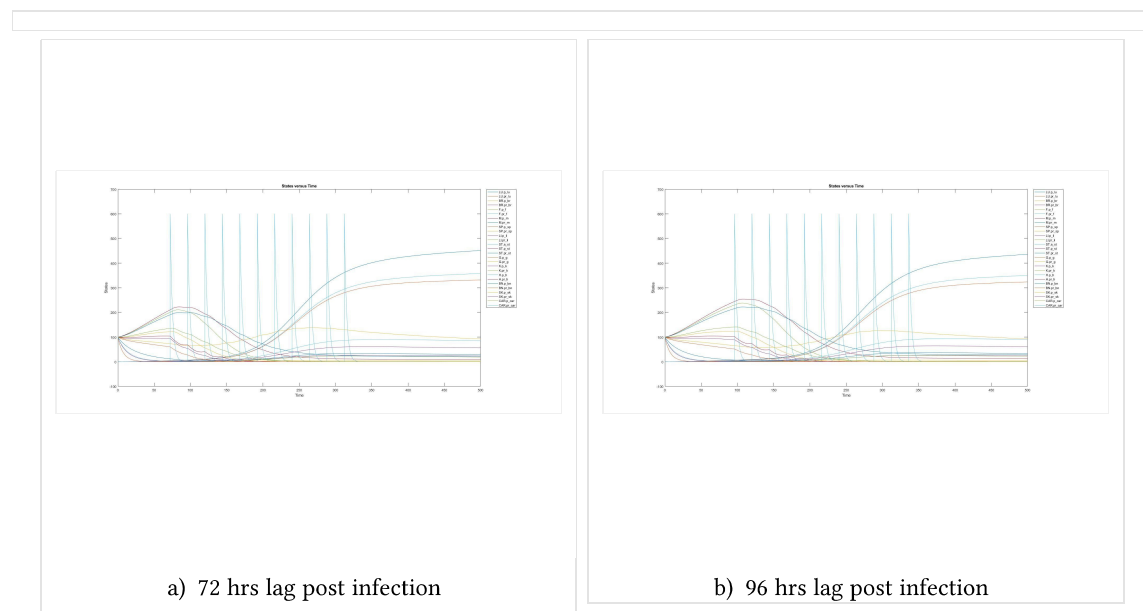


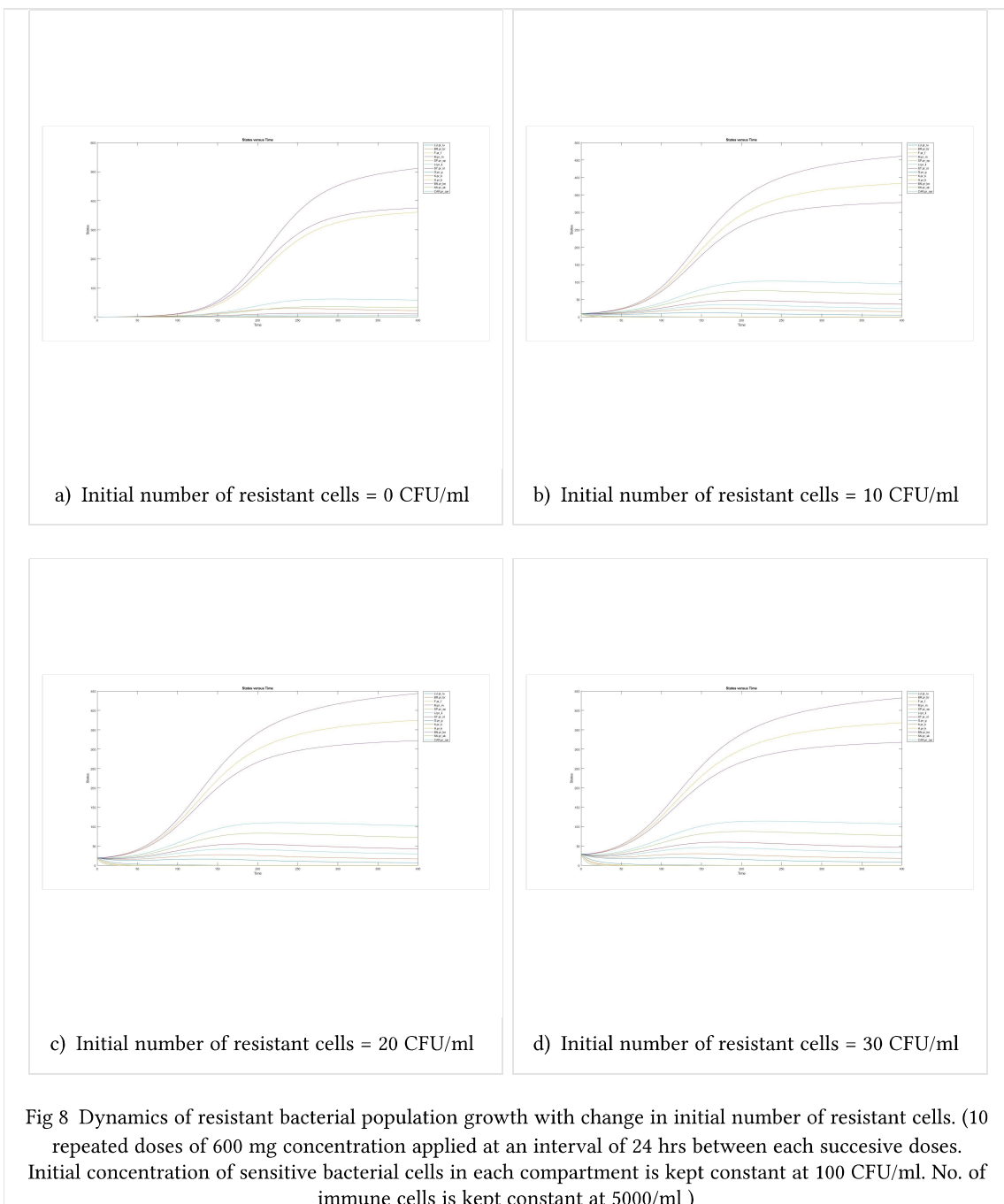
Fig 7 Effect on the growth of the bacterial population when the initial dosage is applied at a time lag post-onset of infection. (10 repeated doses of 600 mg concentration applied at an interval of 24 hrs between each successive doses. The initial concentration of sensitive and resistant bacterial cells in each compartment is kept constant at 100 CFU/ml and 0 CFU/ml respectively. No. of immune cells is kept constant at 5000/ml)

Inference

BBased on experimental observation on the parameters used, the duration of log-phase growth of the bacterial cells with the limitation of a maximum threshold concentration of 1500 CFU/ml is estimated to be close to 72 hrs. Thus, a time lag of 72 hrs or more in the first dose of Rifapentine allows the bacterial cells to reach the steady-state population at the stationary phase of growth and exhibit elevated symptomatic effects, further worsening the health of the infected patient. This also leads to accumulation of a gene pool of resistant cells in all compartment which may reach the stationary phase of growth at the onset of treatment and thus cause treatment failure and result in occurrence of chronic symptoms for the disease.

4.2.3 Dynamics of growth of resistant population with change in the initial number of resistant cells

The results obtained are as follows :



Inference

In some bacterial colonies, mutations are occasionally pre-determined with a small section of population primitively and hereditarily resistant to the antibiotic effect of certain drugs and physical treatment methods. This occasionally leads to treatment failure in case of single-drug treatment procedures as complete decay of sensitive cells with elevated drug and immune levels are not sufficient in the elimination of the entire gene-pool of resistant cells. Along with the complementary effect of mutation of sensitive cells to resistant cells, this allows a decrease in the duration of lag phase, such that the stationary phase of growth is reached at a faster rate, with the appearance of symptomatic effect in all organs.

5 CONCLUSION AND RECOMMENDATIONS

5.1 Conclusion

Based on the assessment of multiple simulations under different reaction conditions, multiple drug dosage regime can be established to eliminate the population of sensitive cells in all the different compartments. A major restriction to this estimation is the difficulty in determination of the extent of infection and spread in different organs of the infected individual. Drugs often carry secondary effects that may harm the human body in terms of retardation of tissue metabolism or deficiency in signalling and transport processes and lead to toxicity. Hence, while devising an optimum drug dosage schedule care must be taken to avoid drug abuse via overconsumption. Also, a lower intake would not allow sufficient absorption of the drug into tissue and may cause some strains of bacteria to survive and produce its phenotypic effects. For an initial population of 100 CFU/ml, an effective dosage regime that can be suggested is as follows:

Table 2 A dosage regime (with initial population at 100 CFU/ml)

Drug dose concentration (Rifapentine)	850mg
Minimum number of repetitions	7
Interval between each successive drug dosage	24 hours

The graph obtained after simulation of the following regime is shown in the figure below :

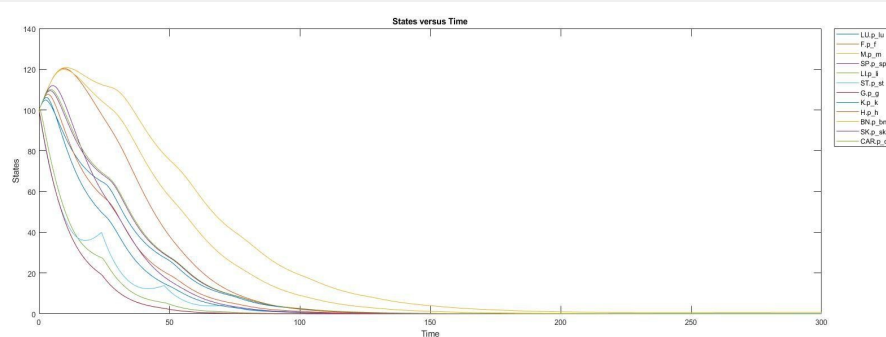


Fig 9 7 doses of 850mg with repetitions of one dose every 24 hours

Although permanent decay of the entire sensitive population may be possible through effective treatment, a very small fraction of bacterial cells might still survive the drug effects by acquiring resistance via mutation. To prevent the emergence of resistant strains, as shown from the simulations, a very strong immune response is necessary to complement the drug effect and produce better treatment results.

5.2 Drawbacks

- Due to limited or no availability of data on various levels of tolerant and resistant Mycobacterium species and their respective parameters of growth, the study of the same is excluded from this research.
- This is a simple model based on an ideal estimate of course of adsorption, distribution, metabolism and excretion (ADME) of a drug. Most of the data are estimated based on the trend observed in general for different Mycobacterium species. The initial concentration of bacterial species and parameters of growth in all compartments are taken to be equal and variance of the same based on the niche of bacterial growth and accessibility of respective compartments are ignored. Thus, there is a major scope of improvement which lies in research carried out in future to accurately evaluate the parameters for bacterial growth for better simulation of growth-kill curves and resistance development.

5.3 Scope for future research

- Modelling persistence/dormancy of the bacterial population and analyse how it responds to change in drug concentration and immunity.
- Modelling treatment to multiple drug and dynamics of Multi-Drug Resistant (MDR) Tuberculosis.
- Segregating the wild type population into different levels of sensitive and tolerant cells.
- Further segregation of resistant population into different levels based on mutation rate and

- interaction with immune cells.
- Segregating the action of immune cells into the contribution of each of its type to the immune response.
- Modelling the dynamics of bacterial response to a different drug.
- The model can be further modified and developed to analyse the dynamics for the action of bacteriophages as antibiotics on disease treatment instead of synthetic drugs.

REFERENCES

1. Sridhar, A., et al. "Fatal poisoning by isoniazid and rifampicin." *Indian journal of nephrology* 22.5 (2012): 385.
2. Bock, Naomi N., et al. "A prospective, randomized, double-blind study of the tolerability of rifapentine 600, 900, and 1,200 mg plus isoniazid in the continuation phase of tuberculosis treatment." *American journal of respiratory and critical care medicine* 165.11 (2002): 1526-1530.
3. Schechter, Mauro, et al. "Weekly rifapentine/isoniazid or daily rifampin/pyrazinamide for latent tuberculosis in household contacts." *American journal of respiratory and critical care medicine* 173.8 (2006): 922-926.
4. Zhang, Fan, et al. "Whole-body physiologically based pharmacokinetic model for nutlin-3a in mice after intravenous and oral administration." *Drug Metabolism and Disposition* 39.1 (2011): 15-21.
5. Zurlinden, Todd J., Garrett J. Eppers, and Brad Reisfeld. "Physiologically Based Pharmacokinetic Model of Rifapentine and 25-Desacetyl Rifapentine Disposition in Humans." *Antimicrobial agents and chemotherapy* 60.8 (2016): 4860-4868.
6. Lyons, Michael A., et al. "A physiologically based pharmacokinetic model of rifampin in mice." *Antimicrobial agents and chemotherapy* 57.4 (2013): 1763-1771.
7. Zhang, Fan, et al. "Whole-body physiologically based pharmacokinetic model for nutlin-3a in mice after intravenous and oral administration." *Drug Metabolism and Disposition* 39.1 (2011): 15-21.
8. Regoes, Roland R., et al. "Pharmacodynamic functions: a multiparameter approach to the design of antibiotic treatment regimens." *Antimicrobial agents and chemotherapy* 48.10 (2004): 3670-3676.
9. Wiuff, C., et al. "Phenotypic tolerance: antibiotic enrichment of noninherited resistance in bacterial populations." *Antimicrobial agents and chemotherapy* 49.4 (2005): 1483-1494
10. Ankomah, Peter, and Bruce R. Levin. "Exploring the collaboration between antibiotics and the immune response in the treatment of acute, self-limiting infections." *Proceedings of the National Academy of Sciences* 111.23 (2014): 8331-8338.
11. Windels, Etthel Martha, et al. "Bacterial persistence promotes the evolution of antibiotic resistance by increasing survival and mutation rates." *ISME J* (2019).
12. Davies, Julian, and Dorothy Davies. "Origins and evolution of antibiotic resistance." *Microbiol. Mol. Biol. Rev.* 74.3 (2010): 417-433.
13. zur Wiesch, Pia Schulz, Jan Engelstädtter, and Sebastian Bonhoeffer. "Compensation of fitness costs and reversibility of antibiotic resistance mutations." *Antimicrobial agents and chemotherapy* 54.5 (2010): 2085-2095.
14. Fisher, Robert A., Bridget Gollan, and Sophie Helaine. "Persistent bacterial infections and persister

- cells." *Nature Reviews Microbiology* 15.8 (2017): 453.
15. Sebastian, Jees, et al. "De novo emergence of genetically resistant mutants of *Mycobacterium tuberculosis* from the persistence phase cells formed against antituberculosis drugs in vitro." *Antimicrobial agents and chemotherapy* 61.2 (2017): e01343-16.
16. Ankomah, Peter, and Bruce R. Levin. "Two-drug antimicrobial chemotherapy: a mathematical model and experiments with *Mycobacterium marinum*." *PLoS pathogens* 8.1 (2012): e1002487.
17. Telenti, Amalio, et al. "Detection of rifampicin-resistance mutations in *Mycobacterium tuberculosis*." *The Lancet* 341.8846 (1993): 647-651.
18. Gillespie, Stephen H. "Evolution of drug resistance in *Mycobacterium tuberculosis*: clinical and molecular perspective." *Antimicrobial agents and chemotherapy* 46.2 (2002): 267-274
19. Gomez, James E., and John D. McKinney. "*M. tuberculosis* persistence, latency, and drug tolerance." *Tuberculosis* 84.1-2 (2004): 29-44.

ACKNOWLEDGEMENTS

I'm extremely grateful to the Indian Academy of Sciences to provide me with the golden opportunity for a summer research project under the guidance of Dr Chetan J Gadgil at NCL, Pune. Further, I am eternally grateful to my guide for giving me an opportunity to work in his lab, for teaching me new concepts, showing research procedures and helping me in every step of my project. I am also thankful to all of my labmates, the PhD students and my fellow interns who guided me in my work. I would also like to thank AuthorCafe for providing such a wonderful platform to write my project report.

APPENDICES

The PBPK model

The equations governing the PBPK model is given as follows :

Stomach :

$$\frac{dA_{ST}}{dt} = F_a D \cdot d(t) - k_{SG} A_{Stomach}^{RPT} \quad \text{where} \quad F_a = \frac{F_{a,k}}{F_{a,k} + D} \quad \text{and} \quad k_{SG} = \text{Gut lumen absorption rate}$$

Gut :

$$\frac{dA_G^{RPT}}{dt} = Q_G (C_{A,f}^{RPT} - C_{G,ven}^{RPT}) + k_{GLG} A_{GL}^{RPT} + k_{SG} A_{RPT}^{stom}$$

Gut Lumen :

$$\frac{dA_{GL}}{dt} = (1 - f_R) \cdot CL \cdot (Q_{LA} C_A + Q_S C_{VS} + Q_G C_{VG}) / Q_L - k_{GLG} A_{GL} - k_F A_{GL}$$

Liver :

$$\frac{dA_L}{dt} = Q_{LA} C_A + Q_S C_{VS} + Q_G C_{VG} - Q_L C_{VL} - (1 - f_R) \cdot CL \cdot (Q_{LA} C_A + Q_S C_{VS} + Q_G C_{VG}) / Q_L - \mu$$

$$\text{where } \mu = \frac{v_M C_{Liver}^{RPT}}{K_M + C_{Liver}^{RPT} + \frac{(C_{Liver}^{RPT})^2}{K_I}}$$

Kidney :

$$\frac{dA_K}{dt} = Q_K (C_{A,f}^{RPT} - C_{K,Ven}^{RPT}) - f_R \cdot CL^{RPT} \cdot C_{A,f}^{RPT}$$

Lung :

$$\frac{dA_{lung}}{dt} = Q_C (C_{V,venous}^i - C_{L,ven}^i) \quad \text{where} \quad i = RPT/dRPT$$

Brain, Bone, Skin, Spleen :

$$\frac{dA_t}{dt} = Q_t (C_{A,f}^{RPT} - C_{T,Ven}^{RPT})$$

Arteries :

$$\frac{dA_A}{dt} = Q_C (C_{L,ven}^i - C_{A,f}^i) \quad \text{where} \quad i = RPT/dRPT$$

Veins :

$$\frac{dA_V}{dt} = \sum_t Q_T C_{VT} - Q_C C_V$$

There is a constant input of drug into the organ through the artery and a constant output of drug from the organ to veins except for lungs where blood flow from vein acts as input and flow of blood to artery acts as output. Hepatic clearance or the amount of drug entering the hepatocytes and getting cleared through metabolism is modelled in terms of Michelis-Menten's reaction kinetics. Further, biliary excretion of the drug occurs from the hepatocyte to the gut through bile which is followed by partial intestinal reabsorption of the drug through the gut mucosal lining. Some part of the drug is removed from the kidney as renal clearance

and excreted through urine. Also, a fraction of the drug doesn't get absorbed and is removed as faecal matter.

PARAMETER	DESCRIPTION	VALUES
Kp_lu	Partition coefficient for Lungs	29.384
Kp_br	Partition coefficient for Brain	3.56
Kp_f	Partition coefficient for Fats	47.895
Kp_m	Partition coefficient for Muscle	22.807
Kp_sp	Partition coefficient for Spleen	29.973
Kp_li	Partition coefficient for Liver	110.051
Kp_g	Partition coefficient for Gut	68.696
Kp_k	Partition coefficient for Kidney	53.212
Kp_h	Partition coefficient for Heart	38.315
Kp_bn	Partition coefficient for Bone	16.978
Kp_sk	Partition coefficient for Skin	50.793
Kp_car	Partition coefficient for Carcass	29.972
Qtot	Cardiac Output	370.85 liter/hour
fB	Fraction bound (fraction of drug bound to blood plasma)	0.994
Fak	Fractional absorption constant	21.23 milligram/kilogram
Ksg	Oral absorption rate	0.33 hr ⁻¹
Klgg	Gut lumen reabsorption	0.17 hr ⁻¹
CLb	Total blood clearance (Renal clearance)	(Variable) liter/hour
fR	Fractional renal clearance	0.13
Vmax	Maximum reaction velocity scaled to body weight (Liver metabolism)	(Variable) micromole/hour
Km	Michaelis-Menten's reaction constant (Metabolism)	34.29 micromole/liter
KI	Rate constant for metabolism	168.07 micromole/liter
Wt	Weight of the individual	65 Kg
D	Dosage amount	13.84 mg/kg
Wt_rif	Molar mass of Rifapentine	0.877 milligram/micromole
Qbr	Flow rate of blood to the brain	(Variable) liter/hour
Qf	Flow rate of blood to the fat tissue	(Variable) liter/hour
Qm	Flow rate of blood to the muscles	(Variable) liter/hour
Qsp	Flow rate of blood to the spleen	(Variable) liter/hour
Qli	Flow rate of blood to the liver	(Variable) liter/hour
Qg	Flow rate of blood to the gut	(Variable) liter/hour
Qsk	Flow rate of blood to the skin	(Variable) liter/hour

Qh	Flow rate of blood to the heart	(Variable) liter/hour
Qk	Flow rate of blood to the kidney	(Variable) liter/hour
Qbn	Flow rate of blood to the bone	(Variable) liter/hour
Qcar	Flow rate of blood to the carcass	(Variable) liter/hour
Ke	Drug excretion rate constant from the liver	0.8 hr ⁻¹
Vlu	Fractional compartmental volume of lungs	0.0076 liter/kg
Vbr	Fractional compartmental volume of brain	0.02 liter/kg
Vf	Fractional compartmental volume of fat tissue	0.2142 liter/kg
Vm	Fractional compartmental volume of muscles	0.4 liter/kg
Vsp	Fractional compartmental volume of spleen	0.0026 liter/kg
Vli	Fractional compartmental volume of liver	0.0257 liter/kg
Vg	Fractional compartmental volume of gut	0.0171 liter/kg
Vh	Fractional compartmental volume of heart	0.0047 liter/kg
Vk	Fractional compartmental volume of kidney	0.0044 liter/kg
Vsk	Fractional compartmental volume of skin	0.0371 liter/kg
Vbn	Fractional compartmental volume of bone	0.1429 liter/kg
Vcar	Fractional compartmental volume of carcass	0.0448 liter/kg
Var	Fractional compartmental volume of artery	0.0263 liter/kg
Vven	Fractional compartmental volume of veins	0.0526 liter/kg
Vst	Fractional compartmental volume of stomach	(Not mentioned) liter
v	Reaction velocity (Liver metabolism)	0.97 micromole/hour
Fa	Fraction of the drug absorbed	(Variable)
d(t)	Oral dose rate	(Variable) micromole/hour
a_st	Oral dosage / Amount of drug ingested	(Variable) milligram
c_plasma	Concentration of unbound drug in plasma	(Variable) milligram/liter
c_lu	Concentration of drug in the lungs	(Variable) milligram/liter
c_br	Concentration of drug in the brain	(Variable) milligram/liter
c_f	Concentration of drug in the fat tissues	(Variable) milligram/liter
c_m	Concentration of drug in the muscle	(Variable) milligram/liter
c_sp	Concentration of drug in the spleen	(Variable) milligram/liter
c_li	Concentration of drug in the liver	(Variable) milligram/liter
c_g	Concentration of drug in the gut	(Variable) milligram/liter
c_k	Concentration of drug in the kidney	(Variable) milligram/liter
c_h	Concentration of drug in the heart	(Variable) milligram/liter
c_bn	Concentration of drug in the bone	(Variable) milligram/liter
c_sk	Concentration of drug in the skin	(Variable) milligram/liter
c_car	Concentration of drug in the carcass	(Variable) milligram/liter
c_ar	Concentration of drug in the artery	(Variable) milligram/liter

c_ven	Concentration of drug in the vein	(Variable) milligram/liter
-------	-----------------------------------	----------------------------

The data on each of the above parameters are obtained from the model by Zurlinden et. al. (4).

The species simulated for the pharmacodynamic action of the drug are :

COMPARTMENT	SPECIES	SPECIES DESCRIPTION
Lungs	LU.p_lu	Population of sensitive species
	LU.pr_lu	Population of resistant species
	LU.c_br	Concentration of drug in the compartment
Brain	BR.p_br	Population of sensitive species
	BR.pr_br	Population of resistant species
	BR.c_br	Concentration of drug in the compartment
Fats	F.p_lu	Population of sensitive species
	F.pr_lu	Population of resistant species
	F.c_lu	Concentration of drug in the compartment
Muscle	M.p_m	Population of sensitive species
	M.pr_m	Population of resistant species
	M.c_m	Concentration of drug in the compartment
Spleen	SP.p_sp	Population of sensitive species
	SP.pr_sp	Population of resistant species
	SP.c_sp	Concentration of drug in the compartment
Liver	LI.p_li	Population of sensitive species
	LI.pr_li	Population of resistant species
	LI.c_li	Concentration of drug in the compartment
Stomach	ST.p_st	Population of sensitive species
	ST.pr_st	Population of resistant species
	ST.a_st	Amount of drug ingested
Gut	G.p_g	Population of sensitive species
	G.pr_g	Population of resistant species
	G.c_g	Concentration of drug in the compartment
Kidney	K.p_k	Population of sensitive species
	K.pr_k	Population of resistant species
	K.c_k	Concentration of drug in the compartment
Heart	H.p_h	Population of sensitive species
	H.pr_h	Population of resistant species

	H.c_h	Concentration of drug in the compartment
Bone	BN.p_bn	Population of sensitive species
	BN.pr_bn	Population of resistant species
	BN.c_bn	Concentration of drug in the compartment
Skin	SK.p_sk	Population of sensitive species
	SK.pr_sk	Population of resistant species
	SK.c_sk	Concentration of drug in the compartment
Carcass	CAR.p_car	Population of sensitive species
	CAR.pr_car	Population of resistant species
	CAR.c_car	Concentration of drug in the compartment